30th Annual International IEEE EMBS Conference
Vancouver, British Columbia, Canada, August 20-24, 2008

Semi-Automatic Detection of the Left Ventricular Border

Maria do Carmo dos Reis, Adson F. da Rocha, Daniel F. Vasconcelos, Bruno L. M. Espinoza, Francisco A. de O. Nascimento, João L. A. de Carvalho, Sauro Salomoni and Juliana F. Camapum

Abstract— **Two semi-automatic methods for the detection of the left ventricular border in two-dimensional short axis echocardiographic images are presented and compared. In these methods, the left ventricular area variation curve is calculated during a complete cardiac cycle after the segmentation of several frames. This allows the evaluation of the cardiovascular dynamics and the identification of important clinical parameters. The algorithms are proposed as several independent modules. The results are validated through the comparison between the semi-automatic continuous boundaries and manuals boundaries sketched by a medical specialist.**

***Keywords*: segmentation, echocardiographic images, motion estimation, area variation, boundary detection.**

I. Introduction

THE analysis of two-dimensional echocardiographic images for the assessment of myocardial function requires the identification of the left ventricle walls. Some clinical parameters can be calculated after the segmentation and detection of the left ventricle border during the end-diastole and end-systole in order to assist the specialist in the diagnosis of cardiac diseases. Several methods have been proposed with the aim of left ventricle boundary detection [1-9]. However, there is still room for innovation and improvement of these methods and algorithms. Some of these works use short axis images [3,7,9] and others focus on long axis images [4,5]. There are semi-automatic algorithms [6,7] and also those that provide fully automated detection [1,5,8].

In the method discussed above, many techniques are used in the image pre-processing stage, such as morphological filtering to reduce noise and improve image contrast [6]. Andrade *et al.* [1] applied the discrete wavelet transform (DWT) to reduce the speckle noise and a second order derivative operator called LoG (Laplacian of the Gaussian) to increase the contrast. Espinoza *et al.* [2] used a pro-mediation filter, which implements temporal averaging of successive frames of the same cardiac cycle.

In this work, two methods for cardiac image segmentation are presented. In the first method, a motion detection procedure is used for rejecting frames with movement. In the second method, the frame rejection step was eliminated, and border extraction was achieved using motion estimation.

In both methods, pre-processing filters are applied to reduce noise and increase contrast. The segmentation of the cardiac cavity is carried through thresholding operation and border extraction by means of neighborhood operations. From the segmented region, the left ventricular area is calculated and the area variation curve of a complete cardiac cycle is determined.

II. Development

A. First Segmentation Method

Fig. 1 shows a diagram of the described algorithm.

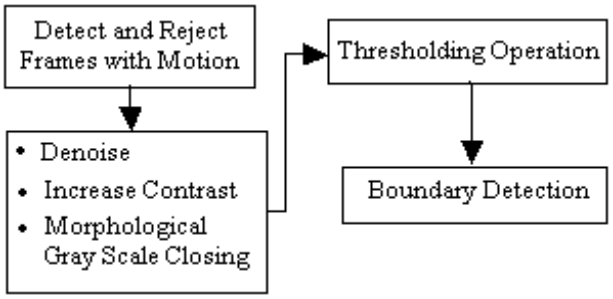

Fig. 1. Diagram of the algorithm of the first method implemented for left ventricular segmentation.

The first step consists of the detection and rejection of frames with movement. Sets of ten consecutive frames are selected in a sliding window fashion (Fig. 2), and the optic flow (OF) for each set is calculated. The OF is calculated by looking for the most likely position where each object from the current frame was located in a previous frame (reference frame). The video frame is partitioned into non-overlapping macro-blocks (MB) of 16x16 pixels and a diamond search scheme is applied. The output of the OF is a motion vector for each MB which represents the object displacement that occurred between current and reference frames (Fig. 3). After movement detection, frames with strong movement are eliminated in order to prevent the degradation of the mean image which is obtained in the following step. The

Manuscript received April 7, 2008.

M. do C. dos Reis, J. F. Camapum, A. F. da Rocha, F. A. de O. Nascimento, B. L. M. Espinoza and S. Salomoni are with the Electrical Engineering Department, University of Brasília, Brasília, DF 70910-900 Brazil (e-mail: carminhamcr@yahoo.com.br, juliana@ene.unb.br, adson@unb.br, assis@unb.br).

D. F. Vasconcelos is with the Medical School and the Electrical Engineering Department, University of Brasília, Brasília, DF 70910-900 Brazil.

J. L. A. Carvalho is with the Department of Electrical Engineering, University of Southern California, Los Angeles, CA 90007, USA.

five frames with stronger movement from each set are eliminated.

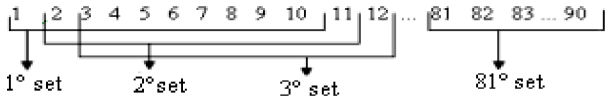

Fig. 2. Sets of ten consecutive frames are selected in a sliding window fashion. The optic flow for each set is calculated as described in Fig. 3.

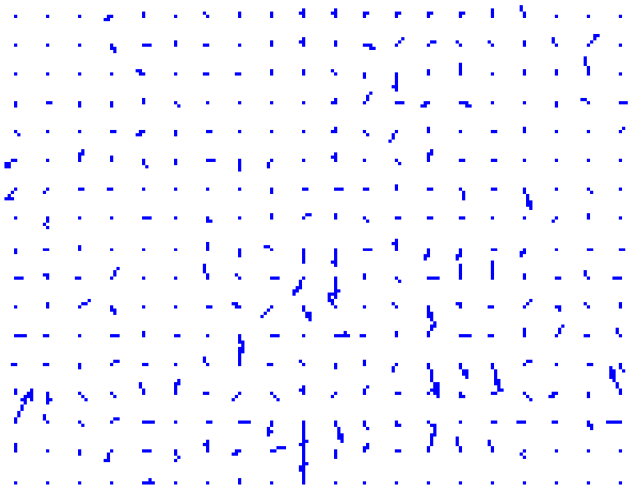

Fig. 3. Optic flow estimation between two consecutive frames.

The second step is the pre-processing stage. This is important for the achievement of an accurate left ventricular border detection, because ultrasound images present strong presence of noise and low contrast. Frequently, these are caused by the physical constitution of the patient, or by the inability in finding the proper acoustical window due to the organ position related to the patient osseous structure [1]. Thus, noise reduction and contrast enhancement operations are used to highlight certain features of interest, which improves the performance of the segmentation step. The pre-processing stage consists in three operations: noise reduction, contrast enhancement, and morphological closing in gray scale. By averaging the remaining five (noisy) frames of each set from step 1, the noise content is reduced. The contrast enhancement operation is used to highlight the intensity difference between the cavity pixels and the muscle walls pixels. In the proposed algorithm, high-boost filtering is used for this operation, which consists in adding a high-pass filtered image to the original image. Next, a Laplacian of the Gausian (LoG) operator is used to further increase contrast while avoiding noise amplification (Fig. 4a). Finally, morphological closing in gray scale is used to obtain a uniform cardiac cavity (Fig. 4b).

The third step is the segmentation stage. Thresholding segmentation was used. First, the image histogram of morphological closing gray scale image is calculated. Using the accumulated histogram, the value of the threshold T is chosen such that 72.7% of the pixels have gray scale level below T. Thus, all pixels with intensity greater than or equal to T receive the value 1 (white) and pixels with intensity below T receive the value 0 (black). This threshold value was selected experimentally, and was chosen from probability values between 56% and 72.7%.

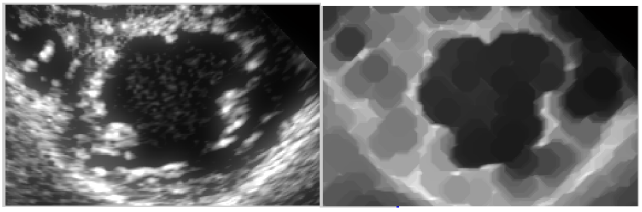

(a) (b)

Fig. 4. (a) Result from high-boost filtering followed by the LoG filtering, (b) Result from morphological closing in Gray scale.

The final step is a boundary detection stage. First, the negative of the thresholded image (Fig. 5b) is calculated in order to transform the ventricular cavity into an object. The image is then scanned pixel by pixel to find and label each connected component. Fig. 5c presents seven connected components, where the second largest region was identified as the ventricular cavity, and thus its pixels are labeled 1 (white) whereas pixels of the other regions are labeled 0 (black). This effectively provides an object that corresponds to the ventricular cavity. From this binary image, the boundary is extracted by means of neighborhood operations. This step adjusts a pixel to zero if its four connected neighbors are one (1), which detects the boundary pixels. The segmentation boundary is shown on Fig. 5d, superimposed on the original image. It has the important property of being a connected path.

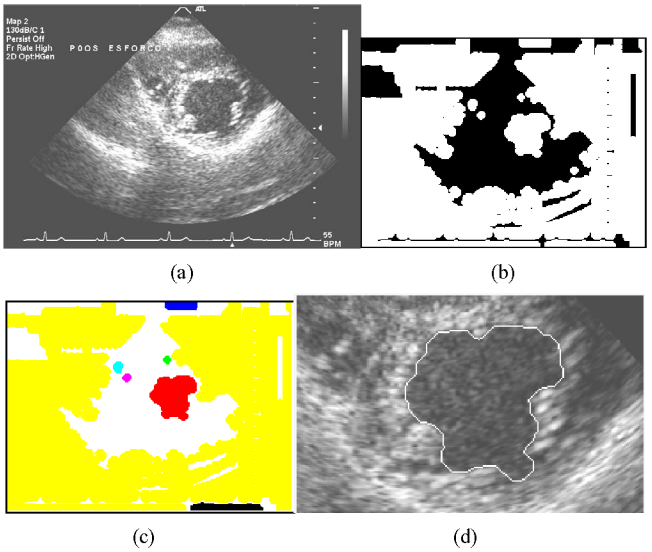

(a) (b)

(c) (d)

Fig. 5. Results from the thresholding operation and boundary detection. (a) Short axis echocardiographic image (b) The negative of the thresholded image, (c) Segmented image with seven labeled connected components, (d) Segmentation boundary of the left ventricular cavity superimposed on the original image.

After the boundary detection, the ventricle area is calculated for each frame, and the area variation curve is constructed (Fig. 6). This curve allows the evaluation of systolic and diastolic ventricular function, the visualization of all stages of the cardiac cycle, the time interval of each of these stages, and the gathering of important information such as area variation fraction or shortening fraction [2].

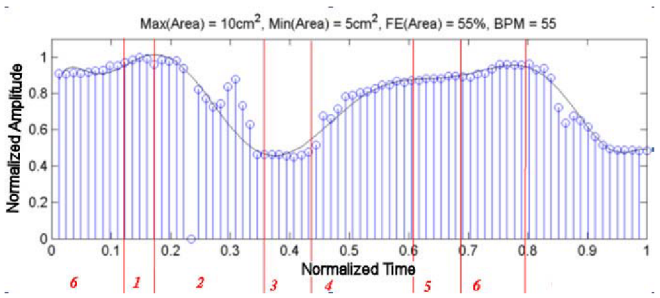

Fig. 6. Cardiac cycle stages in the Variation Area Curve. (1) Isovolumetric Contraction, (2) Ejection, (3) Isovolumetric Relaxation, (4) Rapid Filling, (5) Reduced Filling, (6) Atrial Systole

B. Second Segmentation Method

In this method, the frame rejection step used in method 1 was eliminated, and border extraction is achieved using motion estimation. In the sliding window step, this method uses sets of 5 consecutive frames. The first frame of each set is used as the reference frame for the extraction of the border of the following frames within the same set. The ventricular border of the first frame of each group is extracted using the segmentation approach described in section II.A. Motion estimation information (Fig. 3) is used to locate the border position of the reference frame in each one of the four consecutive frames. The position estimation was performed only for border pixels in order to reduce processing time. Each of the resultant movement vectors (v) of the optic flow is composed of two components in the xy plane, one in the *x-axis* (v_x) and another in the *y-axis* (v_y):

$$f_{out}(x_f, y_f) = f_{in}(x_o + v_x, y_o + v_y) \qquad (1)$$

where, (x_o, y_o) is the coordinate pair of each pixel of the border of the reference frame, (x_f, y_f) is the coordinate pair of the corresponding pixel in the next frame, f_{in} is the border of the reference frame and f_{out} is the next frame with the new border pixels.

The output frame f_{out} is initialized as a zero matrix with the same size of the reference frame. After equation (1) is applied to the input frame, the intensity value (255) of the border pixels (x_o, y_o) are copied to the new corresponding coordinate (x_f, y_f) of the output frame f_{out}. The new boundaries may present imperfections, thus they are corrected by applying two morphological operations: dilation and thinning. The number of consecutive dilations was five, and this was followed by successive thinning operation until a one-pixel border-width was obtained. Other operations were applied to eliminate isolated pixels and to remove pixels connected to the border that were not part of the border. Fig. 7 shows the border from the reference frame and the borders from the four consecutive frames detected by motion estimation.

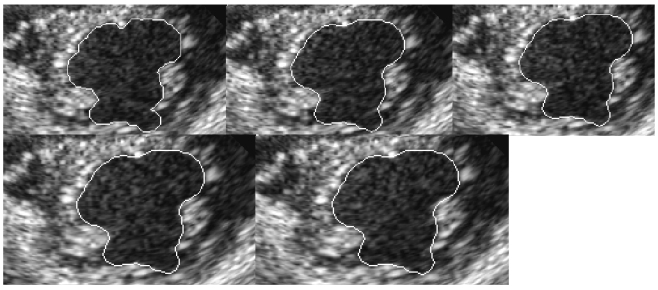

Fig. 7. Examples of boundary detection using motion estimation.

III. Performance Evaluation and Results

In order to evaluate the efficiency of the proposed methods, an image database of 25 images from 13 different patients was created. A medical specialist in the echocardiography area classified these images, based on the contrast and edge appearance, as either high, average, or low quality. Ten images were classified as of high quality, ten images were classified as of average quality, and five images as of low quality. Three index measures were used for the performance evaluation. The first was the linear Correlation Index (CI) between semi-automatically measured areas and manually-segmented measured areas. The second was the Percentile Error (PE), which is the percentile difference between these areas, *i.e.*, the manual non-overlapping area. The third was the Sum Error (SE), which is the percentile sum of the non-overlapping areas. The PE and SE indexes [9] are calculated according to equations (2) and (3), respectively.

$$PE = (|M - A| / M) x100 \qquad (2)$$

$$SE = ((M - A)/M) \times 100 + ((A - M)/M) \times 100 \qquad (3)$$

where, M and A are the inner area of the manual boundary and the semi-automatic boundary, respectively, and (M-A) is the set of pixels that belong to M, but not to A.

The results are shown in Table I. The results from Andrade *et al.* [1] are used as a comparison criterion. These results demonstrate the accuracy of the proposed methods. The high value of the Correlation Index (CI) and the low values of the Percentile Error (EP) and the Sum Error (ES) for the high quality and average quality images show

excellent agreement between manually calculated areas and the semi-automatically calculated areas. In the case of low quality images, the results were not satisfactory. This was predictable, as the specialist cannot manually segment low quality images with accuracy, and therefore such images are typically rejected in practice. The results were statistically similar to those obtained by Andrade *et al.* [1], with smaller standard deviation of percentile and sum errors. This suggests that the proposed methods provide better consistency.

TABLE I
RESULTS OF THE PERFORMANCE EVALUATION FROM THE TWO SEGMENTATION METHODS

	Image Quality – Image Amount	*CI*	*PE (mean ± standard deviation)*	*SE (mean ± standard deviation*
1st method	High - 10	0.95	3.52 ± 1.24	9.47 ± 2.02
	Average - 10	0.90	11.96 ± 3.38	16.49 ± 2.15
	Low - 5	0.68	21.98 ± 7.04	35.50 ± 7.27
2nd method	High - 10	0.94	5.74 ± 2.76	12.44 ± 2.411
	Average - 10	0.90	12.58 ± 3.96	17.99 ± 2.95
	Low – 5	0.68	22.35 ± 8.63	36.25 ± 8.88
High quality long axis echocardiographic images [1]		0,98	2,49 ± 2,46	9,62 ± 7,9

IV. CONCLUSIONS

The proposed methods presented solutions for semi-automatic segmentation of 2D echocardiographic images, combining classic techniques of mathematical morphology for binary images and gray level images, high-boost filtering, image segmentation, and motion estimation. The proposed algorithms provide the area variation curve over a complete cardiac cycle. The automatically-segmented areas show excellent agreement with manually-segmented areas, measured by a specialist. The proposed methods could be used to eliminate inter- and intra-observer variations that are typically observed in manual border delineation.

REFERENCES

[1] M. M. de Andrade, B. L. M. Espinoza, , F. A. de O. Nascimento, A. F. da Rocha, H. S. Carvalho, and P. C. Jesus, "Algoritmo híbrido para segmentação do ventrículo esquerdo em imagens de ecocardiografia bidimensional," *Revista Brasileira de Engenharia Biomédica*, vol. 22, pp. 30-39, 2006.

[2] B. L. M. Espinoza, M. M. de Andrade, F. A. de O. Nascimento, H. S. Carvalho, D. F. Vasconcelos, A. F. da Rocha, and S. A. de Melo Jr., "Algoritmo de segmentação de eco 2D dinâmica," *XXVIII CILAMCE/CMNE (Congresso de Métodos Numéricos em Engenharia)*, Porto, Portugal, vol. 1, pp. 1-16, 2007.

[3] V. Chalana, D. T. Linker, D. R. Haynor, and Yongmin Kim, "A multiple active contour model for cardiac boundary detection on echocardiographic sequences," *IEEE Trans. on Medical Imaging,* vol. 15, n. 3, pp. 290-298, 1996.

[4] Jierong Cheng, Say Wei Foo, and Shankar M. Krishnan, "Automatic Detection of Region of Interest and Center Point of Left Ventricle using Watershed Segmentation," *IEEE Int. Symposium on Circuits and Systems*, vol. 1, n. 2, pp. 149-151, May 2005.

[5] Jierong Cheng, Say Wei Foo, and Shankar M. Krishnan, "Watershed-Presegmented Snake for Boundary Detection and Tracking of Left Ventricle in Echocardiographic Images," *IEEE Trans. on Information Technology in Biomedicine*, vol. 10, n. 2, pp. 414-416, 2006.

[6] M. M. Choy, and S. J. Jesse, "Morphological image analysis of left-ventricular endocardial borders in 2D echocardiograms," *SPIE Proc. on Medical Imaging*, vol. 2710, pp. 852-863, 1996.

[7] J. W. Klingler Jr., C. L. Vaughan, T. D. Fraker Jr., and L. T. Andrews, "Segmentation of echocardiographic images using mathematical morphology," *IEEE Trans. on Biomedical Engineering*, vol. 35, n. 11, pp. 925-934, Nov. 1988.

[8] I. Koren, A. F. Laine, J. Fan, and F. J. Taylor, "Edge detection in echocardiographic image sequences by 3-D multiscale analysis," *in Proc. of the IEEE Int. Conf. on Image Processing*, vol. 1, pp. 288-292, 1994.

[9] A. Laine, and X. Zong, "Border Identification of Echocardiograms via multiscale edge detection and shape modeling," *Proc. of the IEEE Int. Conf. on Image Processing*, vol. 3, pp. 287 - 290 vol.3, Sep. 1996.

[10] P. Lilly, J. Jenkins, and P. Bourdillon, "Automatic Contour Definition on Left Ventriculograms by Image Evidence and a Multiple Template-Based Model," *IEEE Trans. on Medical Imaging*. vol. 8, n. 2, pp. 173-185, 1989.